arXiv:1605.08644v1 [cond-mat.mes-hall] 27 May 2016

Stability of Suspended Graphene under Casimir Force

E. M. Chudnovsky[1] and R. Zarzuela[2]
[1] *Department of Physics and Astronomy, Herbert H. Lehman College, The City University of New York, 250 Bedford Park Boulevard West, Bronx, NY 10468-1589, USA*
[2] *Department of Physics and Astronomy, University of California, Los Angeles, California 90095, USA*

(Dated: March 4, 2024)

We consider graphene sheet suspended above a conducting surface. Treating graphene as an elastic membrane subjected to Casimir force, we study its stability against attachment to the conductor. There exists a critical elevation at the edges below which the central part of suspended graphene nucleates a trunk that becomes attached to the conductor. The dependence of the critical elevation on temperature and dimensions of the graphene sheet is computed.

PACS numbers: 81.05.ue, 46.70.Hg, 03.70.+k

Graphene is a remarkable allotrope of carbon in the form of a honeycomb lattice [1]. This 2D material is expected to mark a major breakthrough in the future of technology due to its unique mechanical, thermal, and electronic properties [2, 3]. Micro-electromechanical systems that involve suspended graphene should take into acount interaction of graphene with surrounding elements. One important source of such interactions is Casimir force between two conducting surfaces that orginates from quantum and thermal fluctuations of the electromagnetic field [4]. It has been intensively studied in recent years in application to graphene heterostructures [5–12].

In the conventional approach to Casimir interactions one studies forces between two surfaces of fixed geometry. Here we take a different approach. We treat suspended graphene as an elastic membrane and consider its deformation due to Casimir forces. Micromechanical studies of elastic membranes have a long history [13]. They have been recently revived in application to graphene [14–17]. In this Letter we are concerned with stability of suspended graphene against attaching to the underlying surface. We show that there exists a critical separation from a conducting surface below which suspended graphene becomes unstable against sagging all the way down to the surface, see Fig. 1.

A 2D elastic membrane is described by energy [13, 14]

$$H_m = \frac{1}{2}\int d^2r\left[\kappa(\boldsymbol{\nabla}^2 h)^2 + \lambda u_{\alpha\alpha}^2 + 2\mu u_{\alpha\beta}^2\right], \quad (1)$$

where $\kappa(T)$ is the flexural stiffness constant, λ and μ are Lamé elastic coefficients, $h(\mathbf{r})$ is the flexural deformation perpendicular to the plane of the membrane, $\mathbf{u}(\mathbf{r})$ is the displacement field in the plane of the membrane, and

$$u_{\alpha\beta} = \frac{1}{2}\left(\partial_\alpha u_\beta + \partial_\beta u_\alpha + \partial_\alpha h \partial_\beta h\right) \quad (2)$$

is the strain tensor. The stress tensor is given by

$$\sigma_{\alpha\beta} = \frac{\delta H_m}{\delta(\partial_\beta u_\alpha)} = \lambda u_{\gamma\gamma}\delta_{\alpha\beta} + 2\mu u_{\alpha\beta}. \quad (3)$$

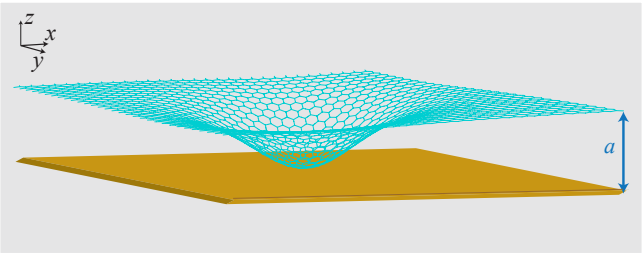


FIG. 1: (Color online) Suspended graphene attracted to a solid surface by Casimir force.

The Euler equations for $\mathbf{u}$ and h are

$$\lambda\partial_\alpha u_{\beta\beta} + 2\mu\partial_\beta u_{\alpha\beta} = 0 \quad (4)$$

$$\kappa\nabla^2\nabla^2 h - \lambda\partial_\alpha(u_{\beta\beta}\partial_\alpha h) - 2\mu\partial_\beta(u_{\alpha\beta}\partial_\beta h) = 0. \quad (5)$$

In a typical experiment a suspended graphene sheet is stretched in the x-direction and held by the edges running in the y-direction. In this case the translational invariance along the y-axis allows one to consider the extremal solutions of Eqs. (4) and (5) that depend on the coordinate x only. This reduces the equations to

$$\partial_x u_{xx} = 0, \quad \partial_x u_{yx} = 0 \quad (6)$$

$$\kappa\partial_x^4 h - (\lambda + 2\mu)\partial_x(u_{xx}\partial_x h) = 0, \quad (7)$$

rendering constant values of u_{xx} and u_{yx} strains. The stress σ in the x-direction generates the strain $u_{xx} \equiv s = \sigma/(\lambda + 2\mu)$. The equation for $h(x)$ then becomes

$$\kappa\partial_x^4 h - \sigma\partial_x^2 h = 0. \quad (8)$$

It can be derived from the effective energy of the membrane

$$H_{\text{eff}} = \int d^2r\left[\frac{\kappa}{2}(\nabla^2 h)^2 + \frac{\sigma}{2}(\nabla h)^2\right] \quad (9)$$

that we will use below.

Before proceeding it is useful to discuss the relative magnitude of the two terms contributing to Eq. (8)

and Eq. (9). From their structure it is clear that the $(\nabla h)^2$ term dominates over the $(\nabla^2 h)^2$ term at curvature radii exceeding $r_c = \sqrt{\kappa/\sigma}$. The typical value of the flexural stiffness constant for graphene is of order $\kappa \sim 1\text{eV}$ ($\sim 10^{-19}\text{J}$). The Lamé coefficients are in the ballpark of 10^2J/m^2 and the typical elastic strain for a suspended graphene sheet is $s \sim 0.001 - 0.01$. This gives $\sigma \sim 0.1 - 1\text{J/m}^2$. Consequently, the critical curvature corresponds to $r_c \sim 1\text{nm}$. We, therefore, conclude that for all effects involving curvature radii in the excess of 1nm the energy of a suspended graphene sheet is dominated by the second term in Eq. (9).

We shall assume that the graphene sheet is suspended above a flat surface of the perfect conductor. The energy of the Casimir attraction per unit area of the graphene sheet at a distance a from the conductor is [5]

$$f = -\frac{U + aV}{16\pi a^3} \tag{10}$$

with

$$U = \hbar c \frac{\alpha N}{8}\left[\ln\left(1 + \frac{8}{\alpha N \pi}\right) + \frac{1}{2}\right], \quad V = k_B T \zeta(3), \tag{11}$$

where $\alpha = (4\pi\epsilon_0)^{-1} e^2/(\hbar c) = 1/137.036 = 7.29735 \times 10^{-3}$ is the fine-structure constant, $N = 4$ is the number of fermion species for graphene, and $\zeta(3) = 1.20205$ is the value of Riemann zeta function $\zeta(x)$ at $x = 3$. The crossover from the low-temperature regime with $f \propto 1/a^3$ to the high-temperature regime with $f \propto 1/a^2$ on increasing separation occurs at

$$\frac{a_t k_B T}{\hbar c} = \frac{\alpha N}{8\xi(3)}\left[\ln\left(1 + \frac{8}{\alpha N \pi}\right) + \frac{1}{2}\right] = 0.01508. \tag{12}$$

For $T = 300\text{K}$ the crossover occurs at $a_t = 115\text{nm}$, while for $T = 4\text{K}$ it occurs at $a_t = 8.63\mu\text{m}$.

We will be interested in a situation when the size of the suspended graphene sheet is large compared to its distance from the underlying surface. The curvature of the graphene sheet will be small so that Eq. (10) for the energy density of Casimir attraction derived for a flat graphene must be approximately valid locally. In this case the total energy can be approximated by $H = H_{\text{eff}} - \int d^2 r f$, that is

$$\begin{aligned} H &= \frac{1}{2}\int d^2 r \left[\kappa(\nabla^2 h)^2 + \sigma(\nabla h)^2\right] \\ &- \beta\hbar c \int d^2 r \left[\frac{1}{(a-h)^3} + \frac{1}{a_t(a-h)^2}\right], \end{aligned} \tag{13}$$

where a is a fixed distance from the conductor at the edges, $h(x, y)$ describes the sagging profile (with $h = 0$ at the edges), and

$$\beta = \frac{\alpha N}{128\pi}\left[\ln\left(1 + \frac{8}{\alpha N \pi}\right) + \frac{1}{2}\right] = 0.0003606235 \tag{14}$$

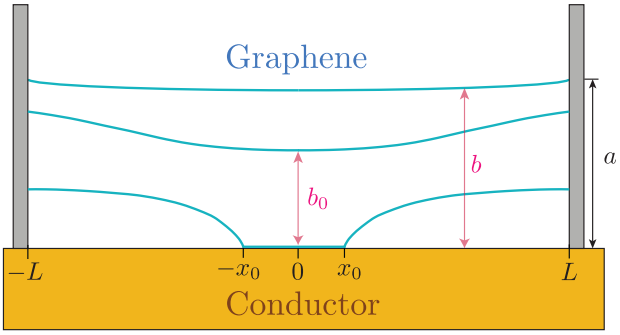


FIG. 2: (Color online) Casimir-driven sagging and instability of a rectangular graphene sheet against attachment to the underlying surface.

$$\begin{aligned} a_t(T) &= \frac{16\pi\beta}{\xi(3)}\frac{\hbar c}{k_B T} = \frac{\alpha N}{8\xi(3)}\left[\ln\left(1 + \frac{8}{\alpha N\pi}\right) + \frac{1}{2}\right]\frac{\hbar c}{k_B T} \\ &= 0.01508\frac{\hbar c}{k_B T}. \end{aligned} \tag{15}$$

The energy (13) is minimized by $h(\mathbf{r})$ satisfying the Euler equation

$$\boldsymbol{\nabla}^2 \frac{\delta H}{\delta \boldsymbol{\nabla}^2 h} - \boldsymbol{\nabla}\frac{\delta H}{\delta \boldsymbol{\nabla} h} + \frac{\delta H}{\delta h} = 0 \tag{16}$$

which gives

$$\left(\kappa\boldsymbol{\nabla}^4 - \sigma\boldsymbol{\nabla}^2\right) h = \beta\hbar c\left[\frac{3}{(a-h)^4} + \frac{2}{a_t(a-h)^3}\right]. \tag{17}$$

Equilibrium sagging profile of a suspended graphene sheet is determined by three factors: The gain in the Casimir energy, the loss in the elastic energy, and the condition $h = 0$ at the boundary. As we shall see below, there is a critical separation at which graphene becomes unstable against attaching to the underlying surface, see Fig. 2. The curvature radius of a suspended graphene must greatly exceed $r_c \sim 1\text{nm}$. This allows one to drop the first term in the left-hand side of Eq. (17). In terms of dimensionless variables

$$\bar{\mathbf{r}} = \frac{\mathbf{r}}{a}, \quad \bar{\boldsymbol{\nabla}} = a\boldsymbol{\nabla}, \quad \bar{h} = \frac{h}{a} \tag{18}$$

the resulting equation is

$$\bar{\boldsymbol{\nabla}}^2 \bar{h} = -\frac{\gamma}{(1-\bar{h})^4} - \frac{\delta_t'}{(1-\bar{h})^3}, \tag{19}$$

where

$$\gamma(a) = 3\beta\frac{\hbar c}{\sigma a^3}, \qquad \delta_t(T) = 2\beta\frac{\hbar c}{\sigma a^2 a_t}. \tag{20}$$

In the low-temperature limit, $a \ll a_t$, Eq. (19) reduces to

$$\bar{\boldsymbol{\nabla}}^2 \bar{b} = \frac{\gamma}{\bar{b}^4} \tag{21}$$

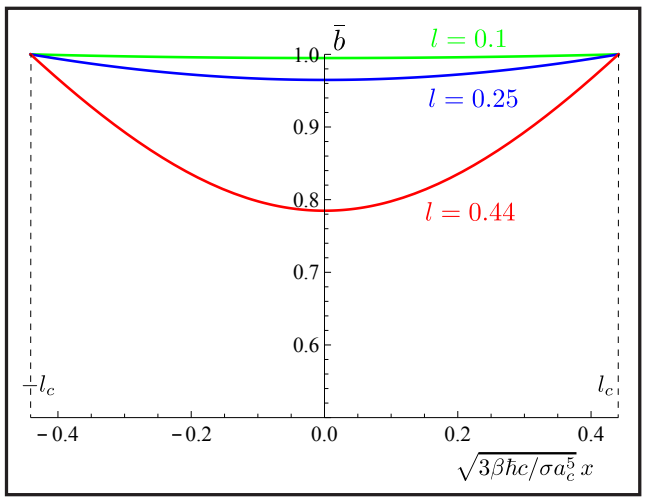


FIG. 3: (Color online) Profile of a sagging graphene due to Casimir force for three values of parameter $l = \gamma^{1/2} L/a$. At $l = 0.1$ the effect of Casimir attraction is weak, while at $l = 0.44$ the graphene sheet is close to the critical separation below which it becomes unstable against sagging all the way down to the conductor.

where $\bar{b} = 1 - \bar{h}$ is the distance from the conductor in the units of a. We consider a rectangular graphene sheet of length $2L$, stretched in the x-direction by walls parallel to the yz-plane. In this case $h = h(x)$ and the first integral of Eq. (21) is

$$\left(\frac{d\bar{b}}{d\bar{x}}\right)^2 = \frac{2\gamma}{3}\left(\frac{1}{\bar{b}_0^3} - \frac{1}{\bar{b}^3}\right), \tag{22}$$

where $\bar{b}_0 < 1$ is the minimal separation of graphene from the conductor at $\bar{x} = 0$. The value of $\bar{b}_0$ must follow from the boundary conditions $\bar{b}(\bar{x} = \pm L/a) = 1$ for the graphene sheet clipped at $x = \pm L$.

The minimal separation at the edges, a_c, before the graphene sheet becomes unstable against attaching to the underlying surface (see Fig. 2) can be estimated from the following argument. The boundary condition, $\bar{b} = 1$ at $x = \pm L$, provides $\left(d\bar{b}/d\bar{x}\right)^2 \sim (1 - \bar{b}_0)^2 (a/L)^2 \sim (2\gamma/3)\left(\bar{b}_0^{-3} - 1\right)$, that is, $(2\gamma/3)\,(L/a)^2 \sim \bar{b}_0^3 (1 - \bar{b}_0)/(1 + \bar{b}_0 + \bar{b}_0^2) < \bar{b}_0 < 1$, which gives $a > a_c \sim 2^{1/5}\,(\beta\hbar c/\sigma)^{1/5}\, L^{2/5}$.

This qualitative analysis is confirmed by numerical solution of Eq. (22) illustrated in Fig. 3. It shows that the strength of the Casimir effect is determined by the parameter $l = \gamma^{1/2} L/a = \sqrt{(3\beta\hbar c)/(a^5\sigma)}\, L$. The sagging profile shown in Fig. 3 exists at $l < l_c = 0.441$. At $l > l_c$ it is unstable against nucleation of a bubble in the central part of the graphene sheet that subsequently attaches to the underlying conductor. The exact numerical result for the critical separation at the edges in the low-temperature limit reads

$$a_c = 1.73\left(\frac{\beta\hbar c}{\sigma}\right)^{1/5} L^{2/5}. \tag{23}$$

Note that at the critical separation one has $a_c/L \ll 1$, that is, the graphene sheet is still close to flat in real space (when unrenormalized units of length are used). This justifies the use of Eq. (13) with the Casimir potential derived for a flat graphene layer. Another important observation is that as the separation at the edges a approaches a_c from above, the minimum critical distance b_0 from the center of the graphene sheet to the underlying surface remains finite, $\bar{b}_0 = b_0/a \to 0.765$.

For, e.g., $2L \sim 2\mu$m and $\sigma \sim 1\text{J/m}^2$, we get from Eq. (23) $a_c \sim 11$nm. For a more macroscopic graphene sheet of $2L \sim 2$mm one obtains $a_c \sim 0.17\mu$m. These values are small compared to a_t at 4K, which justifies the low-temperature approximation used to find the critical separation in Eq. (23).

In the high temperature-limit, $a \gg a_t$, the first integral of Eq. (19) in one dimension is

$$\left(\frac{d\bar{b}}{d\bar{x}}\right)^2 = \delta_t\left(\frac{1}{\bar{b}_0^2} - \frac{1}{\bar{b}^2}\right). \tag{24}$$

The solution is

$$\bar{b}(\bar{x}) = \bar{b}_0\sqrt{1 + \delta_t \bar{x}^2/\bar{b}_0^4}. \tag{25}$$

The boundary conditions $\bar{b}(\pm L/a) = 1$ give the following expression for $\bar{b}_0$

$$\bar{b}_0^2 = \frac{1}{2}\left[1 + \sqrt{1 - 4\delta_t (L/a)^2}\right]. \tag{26}$$

The stability of the solution requires $4\delta_t'(L/a)^2 < 1$, which translates into

$$a > a_c = \left[\frac{\zeta(3) k_{\rm B} T}{2\pi\sigma}\right]^{1/4} L^{1/2}. \tag{27}$$

As a approaches a_c from above, the distance from the graphene sheet to the underlying surface at the center approaches $b_0 = a/\sqrt{2} \approx 0.707a$, which is comparable to $b_0 \approx 0.765a$ in the low-T limit. At $a < a_c$ graphene is unstable against its central part developing a trunk and attaching to the underlying surface, see Fig. 2.

Choosing $2L \sim 2\mu$m, $\sigma \sim 1$ J/m^2 one obtains from Eq. (27) $a_c \sim 5$nm for the critical separation at $T = 300$K. In this case $a_c \ll a_t$ and the high-temperature approximation is not justified. At $2L \gg 2$mm Eq. (27) gives $a_c \sim 0.17\mu\text{m} > a_t = 0.11\mu$m at $T = 300$K. Notice the week dependence of a_c on temperature. This explains why the values of the critical separation in the low and high temperature regimes are similar.

Although one can question whether our model provides a reliable approximation near the points, $x = \pm x_0$, where

graphene attaches to the surface (see Fig. 2), it is worth mentioning that it does contain such mathematical solutions. Notice that they cannot be obtained from Eqs. (21) and (24) because these equations do not permit $b = 0$. However, at small radii of curvature one should use the dominant $\boldsymbol{\nabla}^4 h$ term in Eq. (17), that comes from the first term in Eq. (9). In one dimension this leads to the equation

$$\frac{d^4\bar{b}}{d\bar{x}^4} = -\frac{\gamma'}{\bar{b}^4} - \frac{\delta_t'}{\bar{b}^3}, \tag{28}$$

where

$$\gamma'(a) = 3\beta\frac{\hbar c}{\kappa a}, \qquad \delta_t'(T) = 2\beta\frac{\hbar c}{\kappa a_t(T)}. \tag{29}$$

In the low-temperature regime the relevant partial solution of $d^4\bar{b}/d\bar{x}^4 = -\gamma'/\bar{b}^4$ is

$$\bar{b}(\bar{x}) = \left(\frac{625\gamma'}{264}\right)^{1/5}(\bar{x} - \bar{x}_0)^{4/5}, \quad \bar{x} > \bar{x}_0. \tag{30}$$

In the high-temperature limit the solution of the equation $d^4\bar{b}/d\bar{x}^4 = -\delta_t'/\bar{b}^3$ near $x = x_0$ is

$$\bar{b} = (2\delta_t')^{1/4}(\bar{x} - \bar{x}_0)\ln^{1/4}\left(\frac{1}{\bar{x} - \bar{x}_0}\right), \quad \bar{x} > \bar{x}_0. \tag{31}$$

Since $\delta_t^{1/4} \propto T^{1/4}$ the temperature dependence is week. Notice also the extremely slow divergence of the first derivative, $d\bar{b}/d\bar{x} = (2\delta_t)^{1/4}\ln^{1/4}[1/(\bar{x} - \bar{x}_0)]$ at $\bar{x} \to \bar{x}_0$, in the high-T case as compared to somewhat faster but still slow divergence $\sim 1/(\bar{x} - \bar{x}_0)^{1/5}$ in the low-T case. These observations may be relevant to the problem of exfoliation of graphene. The divergence of the derivative at the separation point is contrary to the perception (derived from watching separation, e.g., of a scotch tape) that the sheet exfoliates parallel to the substrate.

In Conclusion, by treating a suspended graphene sheet as an elastic membrane we have studied its sagging profile due to Casimir attraction to the underlying conductor. Critical separation at which graphene becomes unstable against attachment to the conductor has been computed as a function of temperature and size of the graphene sheet. While our model ignores certain effects such as, e.g., modification of the Casimir force by weak bending of the graphene sheet, it provides a reasonable estimate of the critical separation and can serve as the first approximation to the stability problem. It may also provide some hints regarding exfoliation of graphene which is the primary method of its low-cost mass production [19].

The authors acknowledge valuable discussions with H. Ochoa. RZ thanks Fundación Ramón Areces for a postdoctoral fellowship within the XXVII Convocatoria de Becas para Ampliación de Estudios en el Extranjero en Ciencias de la Vida y de la Materia.

[1] K. S. Novoselov, A. K. Geim, S. V. Morozov, D. Jiang, Y. Zhang, S. V. Dubonos, I. V. Grigorieva and A. A. Firsov, Electric field effect in atomically thin carbon films, Science **306**, 666-669 (2004); K. S. Novoselov, A. K. Geim, S. V. Morozov, D. Jiang, M. I. Katsnelson, I. V. Grigorieva, S. V. Dubonos and A. A. Firsov, Two-dimensional gas of massless Dirac fermions in graphene, Nature **438**, 197-200 (2005).

[2] A. H. Castro Neto, F. Guinea, N. M. R. Peres, K. S. Novoselov, and A. K. Geim, The electronic properties of graphene, Review of Modern Physics **81**, 109-162 (2009).

[3] K. S. Novoselov, V. I. Fal'ko, L. Colombo, P. R. Gellert, M. G. Schwab, and K. Kim, A roadmap for graphene, Nature **490**, 192-200 (2012).

[4] M. Kardar and R. Golestanin, The "friction" of vacuum, and other fluctuation-induced forces, Review of Modern Physics **71**, 1233-1245 (1999).

[5] M. Bordag, I. V. Fialkovsky, D. M. Gitman, and D. V. Vassilevich, Casimir interaction between a perfect conductor and graphene described by the Dirac model, Physical Review B **80**, 245406-(5) (2009); I. V. Fialkovsky, V. N. Marachesvky and D. V. Vassilevich, Finite-temperature Casimir effect for graphene, Physical Review B **84**, 035446-(10) (2011); M. Bordag, I. Fialkovskiy, and D. Vassilevich, Enhanced Casimir effect for doped graphene, Physical Review B **93**, 075414-(5) (2016).

[6] D. Drosdoff and L. M. Woods, Casimir forces and graphene sheets, Physical Review B **82**, 155459-(10) (2010); D. Drosdoff and L. M. Woods, Casimir interactions between graphene sheets and metamaterials, Physical Review A 84, 062501-(7) (2011).

[7] B. E. Sernelius, Casimir interactions in graphene systems, Europhysics Letters **95**, 57003-(4) (2011); B. E. Sernelius, Electromagnetic normal modes and Casimir effects in layered structures, Physical Review B **90**, 155457-(57) (2014).

[8] D. Drosdoff, A. D. Phan, L. M. Woods, I. V. Bonarev, and J. F. Dobson, Effects of spatial dispersion on the Casimir force between graphene sheets, European Physics Journal B **85**, 365-370 (2012).

[9] M. Baibarac, I. Baltog, L. Mihut, I. Pasuk and S. Lefrant, Casimir effect demonstrated by Raman spectroscopy on trilayer graphene intercalated into stiff layered structures of surfactant, Carbon **51**, 134-142 (2013).

[10] A. I. Volokitin and B. M. J. Persson, Influence of electric current on the Casimir forces between graphene sheets, Europhysics Letters **103**, 24002-(6) (2013).

[11] H. Y. Wu and M. Schaden, Perturbative roughness corrections to electromagnetic Casimir energies, Physical Review D **89**, 105003-(27) (2014).

[12] A. A. Banishev, H. Wen, J. Xu, R. K. Kawakami, G. L. Klimchitskaya, V. M. Mostepanenko, and U. Mohideen, Measuring the Casimir force gradient from graphene on a SiO_2 substrate, Physical Review B **87**, 205433-(5) (2013); G. L. Klimchitskaya, V. M. Mostepanenko, and B. E. Sernelius, Two approaches for describing the Casimir interaction in graphene: Density-density correlation function versus polarization tensor, Physical Review B **89**, 125407-(9) (2014); G. L. Klimchitskaya and V. M. Mostepanenko, Comparison of hydrodynamic model

of graphene with recent experiment on measuring the Casimir interaction, Physical Review B **91**, 045412-(5) (2015).

[13] D. R. Nelson and L. Peliti, Fluctuations in membranes with crystalline and hexatic order, Journal de Physique **48**, 1085-1092 (1987).

[14] A. Fasolino, J. H. Los, and M. I. Katsnelson, Intrinsic ripples in graphene, Nature Materials **6**, 858-861 (2007); K. V. Zakharchenko, R. Roldán, A. Fasolino, and M. I. Katsnelson, Self-consistent screening approximation for flexible membranes: Application to graphene, Physical Review B **82**, 125435-(5) (2010); R. Roldán, A. Fasolino, K. V. Zakharchenko, and M. I. Katsnelson, Suppression of anharmonicities in crystalline membranes by external strain, Physical Review B **83**, 174104-(7) (2011); P. L. de Andres, F. Guinea, and M. I. Katsnelson, Bending modes, anharmonic effects, and thermal expansion coefficient in single-layer and multilayer graphene, Physical Review B **86**, 144103-(5) (2012); J. H. Los, A. Fasolino, and M. I. Katsnelson, Scaling Behavior and Strain Dependence of In-Plane Elastic Properties of Graphene, Physical Review Letters **116**, 015901-(5) (2016).

[15] E. Cadelano, P. L. Palla, S. Giordano, and L. Colombo, Nonlinear Elasticity of Monolayer Graphene, Physical Review Letters **102**, 235502-(4) (2009).

[16] D.-B. Zhang, E. Akatyeva, and T. Dumitrica, Bending Ultrathin Graphene at the Margins of Continuum Mechanics, Physical Review Letters **106**, 255503-(4) (2011).

[17] N. Lindahl, D. Midtvedt, J. Svensson, O. A. Nerushev, N. Lindvall, A. Isacsson, and E. E. B. Campbell, Determination of the Bending Rigidity of Graphene via Electrostatic Actuation of Buckled Membranes, Nano Letters **12**, 3526-3531 (2012).

[18] J.-W. Jiang, B.-S. Wang, J.-S. Wang, and H. S. Park, A review on flexural mode of graphene: lattice dynamics, thermal conduction, thermal expansion, elasticity, and nanomechanical resonance, Journal of Physics: Condensed Matter, **27**, 083001-(26) (2015).

[19] M. Yi and Z. Shen, A review on mechanical exfoliation for the scalable production of graphene, Journal of Materials Chemistry A, **3**, 11700-11715 (2015).